Large-N droplets in two dimensions

Dean Lee
Department of Physics, North Carolina State University, Raleigh, North Carolina 27695, USA
(Received 20 December 2005; published 19 June 2006)

Using lattice effective field theory, we study the ground state binding energy of N distinct particles in two dimensions with equal mass interacting weakly via an attractive SU(N)-symmetric short range potential. We find that in the limit of zero range and large N, the ratio of binding energies B_N/B_{N-1} approaches the value 8.3(6).

DOI: 10.1103/PhysRevA.73.063204 PACS number(s): 36.40.−c

I. INTRODUCTION

We consider the ground state of N distinct particles in two dimensions with equal mass interacting weakly via an attractive SU(N)-symmetric short range potential. Since the ground state is completely symmetric this is equivalent to the problem of N weakly-bound identical bosons. The self-bound two-dimensional system with a realistic van der Waals potential is relevant to the properties of adatoms on surfaces. In this work, however, we address the question of what happens as the range of the interaction goes to zero

$$V(\vec{x}_1, \ldots, \vec{x}_N) \to C \sum_{1 \le i < j \le N} \delta^{(2)}(\vec{x}_i - \vec{x}_j). \tag{1}$$

Let B_N be the ground state binding energy of the N-particle system in the zero range limit. The first calculation of B_3/B_2 was given in [1]. The precision of this calculation was improved by [2], and most recently a precise value of $B_3/B_2 = 16.522\,688(1)$ was given in [3]. There have also been studies of the four- and five-particle systems [4–6]. But range corrections for these studies appear to be very large, and the first precise determination of B_4/B_2 in the zero range limit was only recently given in [7], yielding a value of $B_4/B_2 = 197.3(1)$.

The behavior of B_N in the large-N limit was also recently discussed in [3]. They showed that due to the weakening of the attractive coupling at short distance scales, the large-N droplet system could be treated classically. This yielded a prediction for the ratio of the binding energies in the large-N limit

$$\lim_{N \to \infty} \frac{B_N}{B_{N-1}} \simeq 8.567. \tag{2}$$

In [8] the N-particle system for $N \le 7$ was investigated using diffusion Monte Carlo with both a Lennard-Jones potential and a more realistic helium-helium potential. However the results showed that range corrections were too large to allow for a determination of B_N/B_{N-1} for large N.

Although there is no known system of atomic or molecular clusters that displays the physics of the zero range limit for large N, the topic is interesting for several reasons. With recent advances in laser trapping techniques it is now possible to produce many-body quantum systems on a two-dimensional optical lattice. Much of the attention has been devoted to the Bose-Hubbard model with repulsive on-site interactions [9,10], but the weakly attractive N-boson system can also be studied. In that case computational lattice studies such as this would be of immediate relevance. Our system also raises interesting questions about the convergence of effective field theory and the large-N limit. Results of previous numerical studies suggest that it is surprisingly difficult to reach the zero range and large-N limits at the same time. We explore why this is the case and what can be done to overcome some of the difficulties. Similar issues arise in systems of higher-spin fermions in optical traps and lattices. In these systems the competition between short range interactions and large-N effects can determine properties of the ground state, two-particle pairing versus multiparticle clustering [11,12].

In this paper we study the N-particle system using lattice effective field theory. The organization of our paper is as follows. We first discuss the renormalization of the interaction coefficient in the two-particle system. We discuss renormalization in the continuum with a sharp momentum cutoff and then on the lattice. After that we address two features of the large-N limit. The first is a rescaling technique that cancels some of the nonzero range corrections from the ratio B_N/B_{N-1}. The other is an overlapping interaction problem that occurs when many particles lie within a region the size of the range of the potential. We show that this problem can produce large systematic errors that grow with N. The strength of the overlapping interaction must be reduced if we wish to probe zero range physics accurately for large N. We demonstrate one way of doing this which exploits an unusual feature of the discrete Hubbard-Stratonovich transformation [13]. Using lowest-order lattice effective field theory, we compute B_N/B_{N-1} for $N \le 10$. Extrapolating to the limit $N \to \infty$, we find the result

$$\lim_{N \to \infty} \frac{B_N}{B_{N-1}} = 8.3(6). \tag{3}$$

II. TWO-PARTICLE SYSTEM AND RENORMALIZED COUPLING

We begin by reviewing the two-particle system in the continuum formalism with a sharp cutoff, Λ, on the magnitude of the momentum. For a zero range potential

$$V(\vec{x}_1, \ldots, \vec{x}_N) = C \sum_{1 \le i < j \le N} \delta^{(2)}(\vec{x}_i - \vec{x}_j), \tag{4}$$

the diagrams which contribute to two-particle scattering are shown in Fig. 1. We let m be the particle mass. In order that

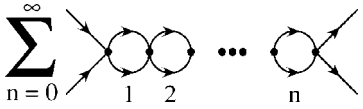

FIG. 1. Diagrams contributing to two-particle scattering for a zero-range potential.

the bound state pole in the rest frame occurs at energy $E=-B_2$, we get the constraint

$$-\frac{1}{C}=\frac{1}{2\pi}\int_0^\Lambda \frac{pdp}{B_2+\frac{p^2}{m}}=\frac{m}{4\pi}\ln\left(\frac{mB_2+\Lambda^2}{mB_2}\right). \tag{5}$$

We can rewrite this as

$$\frac{mB_2\Lambda^{-2}}{1+mB_2\Lambda^{-2}}=\exp\left[\frac{4\pi}{Cm}\right], \tag{6}$$

and the bound state energy is given by

$$mB_2\Lambda^{-2}=\exp\left[\frac{4\pi}{Cm}\right]+O[(mB_2\Lambda^{-2})^2]. \tag{7}$$

We now consider the same calculation on the lattice. Let a be the spatial lattice spacing and a_t be the temporal lattice spacing. We start with the Hamiltonian lattice formulation where $a_t=0$. The standard lattice Hamiltonian with nearest neighbor hopping has the form

$$H=\frac{1}{2ma^2}\sum_{\vec{n}}\sum_{1\le i\le N}\sum_{l=x,y}[2b_i^\dagger(\vec{n})b_i(\vec{n})-b_i^\dagger(\vec{n})b_i(\vec{n}+\hat{l}) - b_i^\dagger(\vec{n})b_i(\vec{n}-\hat{l})]+Ca^{-2}\sum_{\vec{n}}\sum_{1\le i<j\le N}b_i^\dagger(\vec{n})b_i(\vec{n})b_j^\dagger(\vec{n})b_j(\vec{n}). \tag{8}$$

Here, $b_i(\vec{n})$ is an annihilation operator for a particle with flavor i at the spatial lattice site $\vec{n}$. The condition on C in the Hamiltonian lattice formalism is

$$-\frac{1}{C}=\lim_{L\to\infty}\frac{1}{a^2L^2}\sum_{\vec{k}\ \text{integer}}\frac{1}{B_2+2\Omega_{\vec{k}}}, \tag{9}$$

where $\Omega_{\vec{k}}$ is the lattice kinetic energy and L is the length of the periodic lattice cube in lattice units. For the standard lattice action

$$\Omega_{\vec{k}}=\frac{1}{ma^2}\sum_{s=x,y}\left[1-\cos\frac{2\pi k_s}{L}\right]. \tag{10}$$

For later reference we define ω as the momentum independent term inside the summation in (10). So for the standard lattice action $\omega=1$. We define the lattice cutoff momentum $\Lambda=\pi a^{-1}$. Then in the limit $\Lambda\to\infty$

$$mB_2\Lambda^{-2}=B\exp\left[\frac{4\pi}{Cm}\right]+O[(mB_2\Lambda^{-2})^2], \tag{11}$$

where for the standard action $B\simeq 3.24$.

In order to test the cutoff dependence of our lattice results, we also consider actions with $O(a^2)$-improved and $O(a^4)$-improved kinetic energies. $O(a^2)$ and $O(a^4)$ corrections to the interaction are not included since these would entail a significant number of new interactions. Because we are not performing a full $O(a^2)$ or $O(a^4)$ improvement, we do not expect the improved kinetic energy actions to give qualitatively better results than the standard action. However a comparison of the different actions provides an additional check that the results reproduce continuum limit behavior rather than lattice-dependent artifacts. For the $O(a^2)$-improved action the lattice kinetic energy is

$$\Omega_{\vec{k}}=\frac{1}{ma^2}\sum_{s=x,y}\left[\frac{5}{4}-\frac{4}{3}\cos\frac{2\pi k_s}{L}+\frac{1}{12}\cos\frac{4\pi k_s}{L}\right]. \tag{12}$$

In this case $\omega=\frac{5}{4}$ and $B\simeq 1.79$, where B is defined in the asymptotic expression (11). For the $O(a^4)$-improved action

$$\Omega_{\vec{k}}=\frac{1}{ma^2}\sum_{s=x,y}\left[\frac{49}{36}-\frac{3}{2}\cos\frac{2\pi k_s}{L}+\frac{3}{20}\cos\frac{4\pi k_s}{L} - \frac{1}{90}\cos\frac{6\pi k_s}{L}\right], \tag{13}$$

$\omega=\frac{49}{36}$, and $B\simeq 1.54$. As we increase the order of improvement, $\Omega_{\vec{k}}$ more closely approximates the continuum kinetic energy and B approaches the continuum sharp cutoff value of 1.

At nonzero temporal lattice spacing the same diagrams in Fig. 1 contribute to two-particle scattering. A derivation of the Feynman rules at nonzero temporal lattice spacing for the analogous three-dimensional system can be found in [14], as well as a derivation of the bound state pole condition. In two dimensions the strength of the interaction is given by the transfer matrix element

$$(e^{-a_tCa^{-2}}-1)\left(1-\omega\frac{2a_t}{ma^2}\right)^2, \tag{14}$$

while the free lattice propagator has the form

$$\frac{1}{e^{-(2\pi i/L_t)k_0}-1+a_t\Omega_{\vec{k}}}. \tag{15}$$

L_t is the total number of temporal lattice units and k_0 is an integer from 0 to L_t-1.

As we take $L_t\to\infty$, the energy in physical units becomes a continuous variable. Requiring that the bound state pole in the rest frame occurs at energy $E=-B_2$, we get the constraint

$$\frac{1}{\left(1-\omega\frac{2a_t}{ma^2}\right)^2(e^{-a_tCa^{-2}}-1)} = \lim_{L\to\infty}\frac{1}{L^2}\sum_{\vec{k}\ \text{integer}}\frac{1}{e^{a_tB_2}-1+2a_t\Omega_{\vec{k}}-a_t^2\Omega_{\vec{k}}^2}. \tag{16}$$

At nonzero temporal lattice spacing we therefore have

$$mB_2\Lambda^{-2} = B(a_t m^{-1}a^{-2})\exp\left[\frac{4\pi}{C'm}\right] + O[(mB_2\Lambda^{-2})^2], \tag{17}$$

where

$$C' \equiv \frac{a^2}{a_t}\left(1 - \omega\frac{2a_t}{ma^2}\right)^2(1 - e^{-a_t C a^{-2}}). \tag{18}$$

In this case B is a function of $a_t m^{-1}a^{-2}$ and is different for the standard and improved lattice actions. For given values of B_2, a, and a_t, we determine C in the infinite volume limit $L\to\infty$. For $mB_2\Lambda^{-2}$ not too small, roughly 10^{-6} or larger, we use the exact expression (16) for sufficiently large values for L. For smaller values of $mB_2\Lambda^{-2}$ it is more convenient to use the asymptotic expression (17). But once the interaction coefficient C is determined and we proceed to the N-body system, such extremely large lattice volumes are unnecessary. It suffices to consider lattice systems larger than the characteristic size of the N-body droplet. For large N this is many orders of magnitude smaller than the characteristic size of the two-body droplet.

III. RATIOS IN THE LARGE-N LIMIT

It has been suggested that the large-N ground state wave function can be described as a classical distribution [3]. If R_N is the characteristic size of the droplet, the distribution is proportional to $\psi(r/R_N)$ for some function ψ independent of N, and the binding energy B_N is proportional $m^{-1}R_N^{-2}$. In order to determine ψ, one integrates out high energy modes to determine the effective coupling at energy B_N. If this picture of the large-N droplet is correct, then errors due to the finite cutoff momentum Λ appear only in the combination $mB_N\Lambda^{-2}$. Therefore if we measure binding energies while keeping $mB_N\Lambda^{-2}$ fixed, much of the error cancels in the ratio B_N/B_{N-1}. In essence we are using large-N similarity under rescaling to eliminate cutoff errors. If the classical droplet picture is incorrect, then this technique will probably not reduce errors. The issue will be settled when we analyze results of the Monte Carlo simulations.

Let $B_N(\Lambda)$ be the measured binding energy of the N-particle ground state at cutoff momentum Λ. Conceptually it is simplest to regard m and B_2 as fixed quantities while we vary Λ. In the continuum limit

$$\lim_{\Lambda\to\infty} B_N(\Lambda) = B_N. \tag{19}$$

Let $z>0$ be a parameter that measures proximity to the continuum limit,

$$z = mB_N(\Lambda)\Lambda^{-2}. \tag{20}$$

For a given z, we define the cutoff momentum $\Lambda(z,N)$ implicitly so that

$$mB_N(\Lambda(z,N))(\Lambda(z,N))^{-2} = z. \tag{21}$$

We define $f(z)$ as

$$f(z) = \lim_{N\to\infty}\frac{1}{N}\ln[B_N(\Lambda(z,N))/B_N]. \tag{22}$$

$f(z)$ measures the exponential growth of finite cutoff errors with increasing N. We have

$$\lim_{N\to\infty}\left\{\ln\left[\frac{B_N(\Lambda(z,N))}{B_N}\right] - \ln\left[\frac{B_{N-1}(\Lambda(z,N-1))}{B_{N-1}}\right]\right\} = f(z), \tag{23}$$

and so

$$\lim_{N\to\infty}\frac{B_N}{B_{N-1}} = e^{-f(z)}\lim_{N\to\infty}\frac{B_N(\Lambda(z,N))}{B_{N-1}(\Lambda(z,N-1))}. \tag{24}$$

Therefore so long as $|f(z)|\ll 1$, the large-N ratio of binding energies can be measured reliably. Other cutoff errors which do not grow linearly with N will cancel in the ratio

$$\frac{B_N(\Lambda(z,N))}{B_{N-1}(\Lambda(z,N-1))} \tag{25}$$

as we take $N\to\infty$.

In our Monte Carlo lattice simulations it is more convenient to regard m and Λ as fixed quantities while varying B_2. We define $B_2(z,N)$ implicitly by

$$mB_N(B_2(z,N))\Lambda^{-2} = z. \tag{26}$$

We are changing the overall physical scale when we change B_2, and so we work with ratios B_N/B_2. The analog of the result (24) is

$$\lim_{N\to\infty}\frac{B_N}{B_{N-1}} = e^{-f(z)}\lim_{N\to\infty}\frac{B_N(B_2(z,N))/B_2(z,N)}{B_{N-1}(B_2(z,N-1))/B_2(z,N-1)}. \tag{27}$$

IV. OVERLAPPING RANGE AND IMPLICIT N-BODY INTERACTION

Large range corrections can occur when many particles lie within a region the size of the range of the potential, Λ^{-1}. The problem is most severe when all N particles lie in this localized region, and the potential energy is amplified by a factor of $N(N-1)/2$. For a continuum potential with a repulsive core, the result is a deep hole at the center of the multiparticle wave function and a tendency towards underbinding or unbinding. At lowest order in lattice effective field theory the effect goes in the opposite direction. A spike forms at the center of the wave function when all particles lie on the same lattice site, and the binding energy is too large.

Consider the state with N particles at the same lattice site in the Hamiltonian lattice formalism

$$|\Pi^N\rangle = b_1^\dagger(\vec{n})b_2^\dagger(\vec{n})\cdots b_N^\dagger(\vec{n})|0\rangle. \tag{28}$$

The expectation value of the potential energy for this localized state is

$$\langle \Pi^N | V | \Pi^N \rangle = \frac{CN(N-1)}{2a^2}. \tag{29}$$

This potential energy can be regarded as an implicit N-body contact interaction produced by overlapping two-body interactions. In the continuum limit we know that the importance of this N-body contact interaction is suppressed by many powers of the small parameter $z = mB_N\Lambda^{-2}$. However the situation at finite Λ can be quite different from the continuum limit if the potential energy per particle for the localized state $|\Pi^N\rangle$ is as large as the cutoff energy scale

$$\left| \frac{C(N-1)}{2a^2} \right| \gtrsim \frac{\pi^2}{ma^2}. \tag{30}$$

To lowest order in $mB_2\Lambda^{-2}$, the renormalized coupling is

$$C = \frac{4\pi}{m \ln(mB_2\Lambda^{-2})} = \frac{4\pi}{m \ln(mB_N\Lambda^{-2}) - m \ln(B_N/B_2)}. \tag{31}$$

For large N

$$C \simeq \frac{4\pi}{m \ln z - mN \ln \beta}, \tag{32}$$

where

$$\beta = \lim_{N\to\infty} \frac{B_N}{B_{N-1}}. \tag{33}$$

Then

$$-\frac{C(N-1)}{2a^2} \simeq \frac{\pi^2}{ma^2}\left[\frac{2\pi^{-1}}{\ln \beta - \frac{1}{N} \ln z} \right]. \tag{34}$$

In the continuum limit the problem goes away since

$$\frac{1}{\ln \beta - \frac{1}{N} \ln z} \to 0. \tag{35}$$

However the convergence is slow and requires $z \ll e^{-N}$. For actual lattice simulations it is therefore necessary to limit the size of the implicit N-body contact interaction.

V. DISCRETE HUBBARD-STRATONOVICH TRANSFORMATION

There are several ways to deal with the large implicit N-body contact interaction. On the lattice there is one method which is particularly convenient. This is to write the two-body interaction using a discrete Hubbard-Stratonovich transformation [13]. The discrete Hubbard-Stratonovich reproduces the two-body contact interaction exactly. Typically it is used for systems with spin-1/2 fermions where Pauli exclusion implies that there are no N-body contact interactions beyond $N=2$. It seems therefore that the properties of the transformation for $N \geq 3$ has not been discussed in the literature. In the following we show that when a discrete Hubbard-Stratonovich transformation is used, the temporal lattice spacing regulates the strength of the implicit N-body contact interaction.

For simplicity we show only the interaction part of the Hamiltonian. The exponential of the two-body interaction at site $\vec{n}$ over a Euclidean time step a_t is

$$e^{-a_t H_{\rm int}} = \exp\left[-a_t C a^{-2} \sum_{1\leq i<j\leq N} b_i^\dagger(\vec{n}) b_i(\vec{n}) b_j^\dagger(\vec{n}) b_j(\vec{n}) \right]. \tag{36}$$

The discrete Hubbard-Stratonovich transformation amounts to making the replacement

$$e^{-a_t H_{\rm int}} \to \frac{1}{2} \sum_{s(\vec{n})=\pm 1} \exp\left[-\left(\frac{1}{2} a_t C a^{-2} + \lambda s(\vec{n}) \right) \times \left(\sum_{1\leq i\leq N} b_i^\dagger(\vec{n}) b_i(\vec{n}) - 1 \right) \right], \tag{37}$$

where

$$\cosh \lambda = \exp\left(-\tfrac{1}{2} a_t C a^{-2}\right), \quad \lambda \geq 0. \tag{38}$$

To see that this has all the desired properties, let us define

$$A(K) = \frac{1}{2} \sum_{s(\vec{n})=\pm 1} \exp\left[-\left(\tfrac{1}{2} a_t C a^{-2} + \lambda s(\vec{n}) \right)(K-1) \right], \tag{39}$$

for nonnegative integer K. We note that $A(0)=A(1)=1$, and $A(2)=\exp(-a_t C a^{-2})$. These are precisely the expectation values of $e^{-a_t H_{\rm int}}$ for $K=0,1,2$ distinct particles at lattice site $\vec{n}$. When $K \geq 3$ but $\lambda(K-1) \ll 1$, we find

$$A(K) \simeq \exp\left[-a_t C a^{-2} \frac{K(K-1)}{2} \right]. \tag{40}$$

This is also the expectation value of $e^{-a_t H_{\rm int}}$ for K distinct particles at lattice site $\vec{n}$. However when $K \geq 3$ and $\lambda(K-1) \gg 1$

$$A(K) \simeq \tfrac{1}{2} \exp\left[\left(-\tfrac{1}{2} a_t C a^{-2} + \lambda \right)(K-1) \right]. \tag{41}$$

The total potential energy of the K-particle localized state, $|\Pi^K\rangle$, no longer increases quadratically with K. The temporal lattice spacing a_t acts as an auxiliary ultraviolet regulator that limits the size of the implicit K-body contact interaction. When $K \leq 2$ or the implicit K-body contact interaction is smaller than a_t^{-1}, we have the unaltered result

$$\langle \Pi^K | V | \Pi^K \rangle \simeq \frac{CK(K-1)}{2a^2}. \tag{42}$$

When $K > 2$ and the implicit K-body contact interaction exceeds a_t^{-1}, then the regulator takes effect and we have

$$\langle \Pi^K | V | \Pi^K \rangle \simeq a_t^{-1} \left[\left(\tfrac{1}{2} a_t C a^{-2} - \lambda \right)(K-1) + \ln 2 \right]. \tag{43}$$

VI. ALGORITHM

The standard lattice action we use for our simulations is

$$\sum_{\vec{n},n_t,i}\left[c_i^*(\vec{n},n_t)c_i(\vec{n},n_t+1)-e^{-(a_tCa^{-2}/2)-\lambda s(\vec{n},n_t)}\left(1-\frac{2a_t}{ma^2}\right)\right.$$
$$\left.\times c_i^*(\vec{n},n_t)c_i(\vec{n},n_t)\right]-\frac{a_t}{2ma^2}\sum_{\vec{n},n_t,l,i}[c_i^*(\vec{n},n_t)c_i(\vec{n}+\hat{l},n_t)$$
$$+c_i^*(\vec{n},n_t)c_i(\vec{n}-\hat{l},n_t)]-\sum_{\vec{n},n_t}\lambda s(\vec{n},n_t), \quad (44)$$

where n_t is the temporal lattice coordinate, c_i is the path integration field for the particle of type i, and s is the discrete Hubbard-Stratonovich field which takes values ± 1. We have used the lattice conventions developed in [14,15] for a three-dimensional lattice. The choice of Bose or Fermi statistics for c_i is irrelevant since we consider systems with no more than one particle of each type.

In order to compute the ground state binding energy B_N we consider the correlation function

$$Z_N(t)=\langle\Psi_N^0|e^{-Ht}|\Psi_N^0\rangle, \quad (45)$$

where the initial or final state is the state with all N particles at zero momentum

$$|\Psi_N^0\rangle=\tilde{b}_1^\dagger(0)\tilde{b}_2^\dagger(0)\cdots\tilde{b}_N^\dagger(0)|0\rangle. \quad (46)$$

$|\Psi_N^0\rangle$ is also the ground state of the noninteracting system. We refer to t as Euclidean time and define

$$E_N(t)=-\frac{\partial}{\partial t}[\ln Z_N(t)]. \quad (47)$$

Then as $t\to+\infty$, $E_N(t)$ converges to $-B_N$, the ground state energy of the interacting N-particle system. The only assumption is that the ground state has a nonvanishing overlap with the ground state of the noninteracting system.

The conversion of the lattice action to a transfer matrix formalism at fixed particle number has been discussed in [16]. We use the same transfer matrix derived there, except in this case we keep the discrete Hubbard-Stratonovich field and calculate the sum over configurations

$$Z_N(t)\propto\sum_s e^{-\Sigma_{\vec{n},n_t}\lambda s(\vec{n},n_t)}\langle\Psi_N^0|T[e^{-H(s)t}]|\Psi_N^0\rangle, \quad (48)$$

$H(s)$ consists of only single-body operators interacting with the background Hubbard-Stratonovich field. We can write the full N-particle matrix element as the Nth power of the single-particle matrix element

$$\langle\Psi_N^0|T[e^{-H(s)t}]|\Psi_N^0\rangle\propto[M(s,t)]^N, \quad (49)$$

$$M(s,t)=\langle\vec{k}=0|T[e^{-H(s)t}]|\vec{k}=0\rangle, \quad (50)$$

where $|\vec{k}=0\rangle$ is a single-particle state with zero momentum. Our time-ordered exponential notation, $T[e^{-H(s)t}]$, is shorthand for the time-ordered product of single-body transfer matrices at each time step

$$T[e^{-H(s)t}]=M_{(L_t-1)}\cdots M_{(n_t)}\cdots M_{(1)}M_{(0)}, \quad (51)$$

where L_t is the total number of lattice time steps and $t=L_ta_t$. If the particle stays at the same spatial lattice site from time step n_t to n_t+1, then the corresponding matrix element of $M_{(n_t)}$ is

$$e^{-(a_tCa^{-2}/2)-\lambda s(\vec{n},n_t)}\left(1-\frac{2a_t}{ma^2}\right). \quad (52)$$

If the particle hops to a neighboring lattice site from time step n_t to n_t+1 then the corresponding matrix element of $M_{(n_t)}$ is $\frac{a_t}{2ma^2}$. All other elements of $M_{(n_t)}$ are zero.

We sample configurations according to the weight

$$\exp\left\{\sum_{\vec{n},n_t}\lambda s(\vec{n},n_t)+N\ln[M(s,t_{\text{end}})]\right\}, \quad (53)$$

where t_{end} is the largest Euclidean time at which we wish to measure $Z_N(t)$. We use a simple heat bath update procedure. For each configuration the observable that we compute is

$$O(s,t)=\frac{[M(s,t)]^N}{[M(s,t_{\text{end}})]^N}, \quad (54)$$

for $t<t_{\text{end}}$. This is the same general technique that was used in [17]. By taking the ensemble average of $O(s,t)$ we are able to calculate

$$\frac{Z_N(t)}{Z_N(t_{\text{end}})}. \quad (55)$$

VII. RESULTS

For each simulation we have computed roughly 2×10^5 successful heat bath updates for each lattice site, split across four processors running completely independent trajectories. Averages and errors were calculated by comparing the results of each processor. The codes were based on existing codes used for light nuclei in three dimensions and we have kept some of the same input parameters relevant for the light nuclei system. We use a mass of $m=939$ MeV and keep the spatial lattice spacing fixed at $a=(40\text{ MeV})^{-1}$. This corresponds with $\Lambda=\pi a^{-1}\simeq126$ MeV and cutoff energy $\Lambda^2/m=16.8$ MeV. Clearly these input parameters in raw form are not appropriate for atomic clusters. Therefore we translate of all of the parameters in terms of dimensionless numbers which can then be easily applied to any two-dimensional droplet system.

We have already defined the dimensionless ratio z

$$z=\frac{B_N}{\Lambda^2/m}=B_Nma^2\pi^{-2}. \quad (56)$$

z measures the ratio of B_N to the cutoff energy. In most cases it is clear which N we are referring to and so we use the simple notation z. When there is some possibility of confusion we include the N subscript, z_N.

We also define ε

$$\varepsilon=\frac{\pi a_t^{-1}}{\Lambda^2/m}=a_t^{-1}ma^2\pi^{-1}. \quad (57)$$

A small value for ε indicates that there is a significant amount of high frequency regularization provided by the

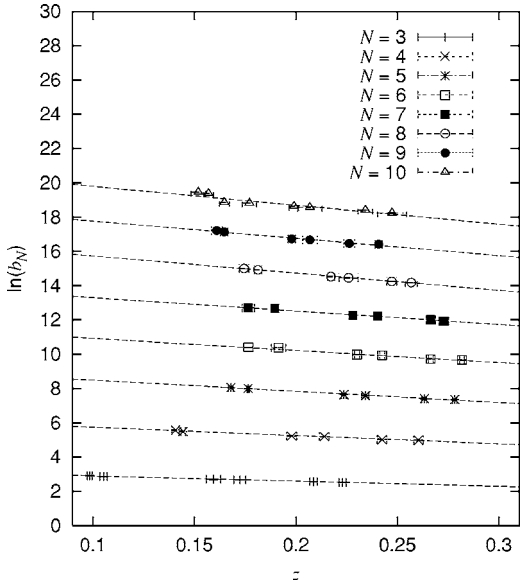

FIG. 2. $\ln(b_N)$ versus z. We use the $O(a^4)$-improved action and $\varepsilon=3.7$.

nonzero temporal lattice spacing a_t. A large value for ε means that we are close to the Hamiltonian limit, $a_t \to 0$. There is little or no regularization of high frequency modes and most of the regularization is provided by the momentum cutoff Λ.

We adjust the two-particle binding energy B_2 in order to study the finite cutoff dependence. Since we keep Λ fixed, our value B_2 will decrease as go to larger values of N. For convenience we use the shorthand

$$b_N = B_N/B_2 \tag{58}$$

for the dimensionless ratio of the binding energies. For each data point we increase the spatial length and temporal extent of the lattice until the finite volume and time errors are clearly smaller than the statistical errors. The largest lattice system we simulate is $9\times9\times260$.

We have computed b_N for $N\leq10$ for a wide range of values for B_2 using the $O(a^4)$-improved action and $a_t=(20\ \mathrm{MeV})^{-1}$, which corresponds with $\varepsilon=3.7$. The results are shown as a plot of $\ln(b_N)$ versus z in Fig. 2. We see that there is considerable dependence on z. The dependence appears to be roughly linear in z for $0.1<z<0.3$, and we have drawn interpolating lines. We note that since $\ln(b_N)$ and $\ln(b_{N-1})$ have approximately the same slope, most of the z dependence cancels in the combination $\ln(b_N)-\ln(b_{N-1})$. This suggests that $f(z)$ as defined in (22) is small. Much of the systematic cutoff errors can be canceled in the ratio b_N/b_{N-1} by keeping z the same for b_N and b_{N-1}. From Fig. 2 we see that b_N/b_{N-1} is about 10 for $5\leq N\leq10$. Therefore scaling B_2 proportional to 10^{-N} as we probe the N-body droplet should keep z approximately the same for these values of N.

Next we calculated b_N/b_{N-1} for $N\leq10$ using three different actions. We compared the standard action, the $O(a^2)$-improved action, and the $O(a^4)$-improved action, using $a_t=(20\ \mathrm{MeV})^{-1}$ and $B_2=2\times10^{2-N}$ MeV. This corresponds with $\varepsilon=3.7$ and $z_2=1.2\times10^{1-N}$. The results are shown in Fig. 3. We see about a 10% variation among the three different actions, with the $O(a^2)$- and $O(a^4)$-improved actions agreeing slightly better with each other than with the standard action.

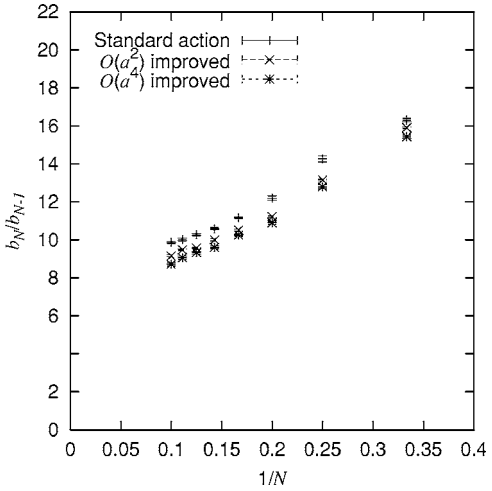

FIG. 3. Comparison of b_N/b_{N-1} for the standard, $O(a^2)$-improved, and $O(a^4)$-improved actions. We use $\varepsilon=3.7$ and $z_2=1.2\times10^{1-N}$.

In Fig. 4 we plot b_N/b_{N-1} using the $O(a^4)$-improved action, $a_t=(20\ \mathrm{MeV})^{-1}$, and three different sets of values for B_2: $B_2=3\times10^{2-N}$ MeV, $2\times10^{2-N}$ MeV, and $1\times10^{2-N}$ MeV. This corresponds with $\varepsilon=3.7$ and $z_2=1.8\times10^{1-N}$, $1.2\times10^{1-N}$, and $0.6\times10^{1-N}$, respectively. The discrepancies for the different values of B_2 are at the 30% level for small N, but as expected the errors decrease with increasing N.

We also studied the dependence of b_N/b_{N-1} on the temporal lattice spacing a_t. We set $B_2=2\times10^{2-N}$ MeV and used the $O(a^4)$-improved action with $a_t=(16\ \mathrm{MeV})^{-1}$, $(20\ \mathrm{MeV})^{-1}$, $(30\ \mathrm{MeV})^{-1}$, and $(40\ \mathrm{MeV})^{-1}$. This corresponds with $z_2=1.2\times10^{1-N}$ and $\varepsilon=3.0$, 3.7, 5.6, and 7.5, respec-

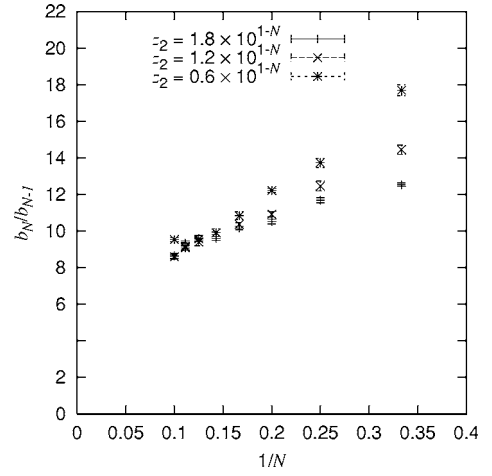

FIG. 4. Comparison of b_N/b_{N-1} for different values of z_2. We use the $O(a^4)$-improved action and $\varepsilon=3.7$.

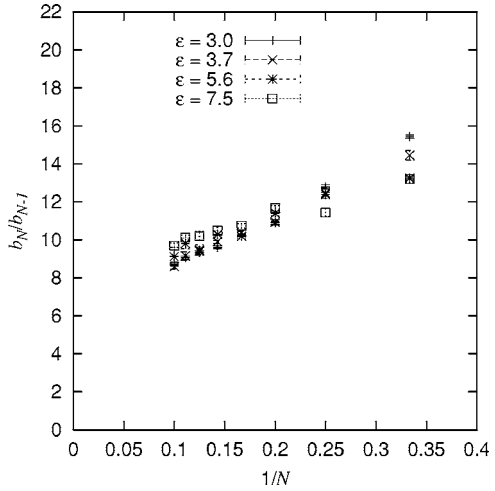

FIG. 5. Comparison of b_N/b_{N-1} for different values of ε. We use the $O(a^4)$-improved action and $z_2=1.2\times10^{1-N}$.

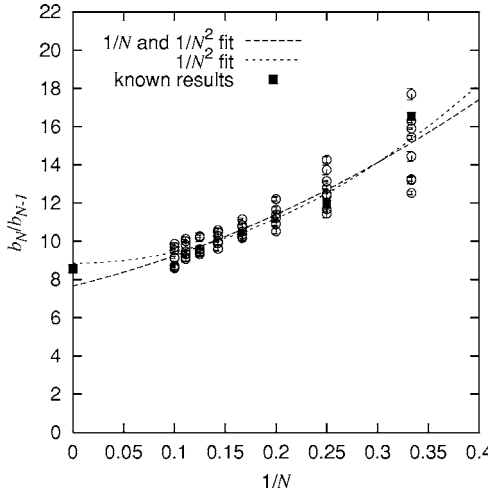

FIG. 6. Cumulative data for b_N/b_{N-1}. We draw two best fit curves with up to quadratic dependence on $1/N$ and show the known results for $N=3$, 4, and ∞.

tively. Since ε is rather large, a_t has only a small effect on the ultraviolet regularization of the two-body interaction. Instead the importance of a_t is as an auxiliary regulator on the implicit N-body contact interaction. The results are shown in Fig. 5. The results appear to differ at about the 10–15% level.

In Fig. 6 we combine all of the data shown in Figs. 3–5. For comparison we include the known results for $N=3$ [3], $N=4$ [7], and $N\to\infty$ [3]. We draw two best fit curves with up to quadratic dependence on $1/N$. The known results were not included in this fit. The best fit curve using $1/N$ and $1/N^2$ gives a value

$$\lim_{N\to\infty}\frac{b_N}{b_{N-1}}\simeq 7.7, \tag{59}$$

while the best fit curve using only $1/N^2$ gives a value

$$\lim_{N\to\infty}\frac{b_N}{b_{N-1}}\simeq 8.8. \tag{60}$$

If we take these two results as approximate lower and upper bounds then we find

$$\lim_{N\to\infty}\frac{b_N}{b_{N-1}}\simeq 8.3(6). \tag{61}$$

VIII. CONCLUSIONS

We have studied the two-dimensional N-particle system with short range attraction using lowest-order lattice effective field theory. We discussed two aspects of the large-N limit. The first is a technique that uses large-N similarity under rescaling to cancel some of the nonzero range corrections from the ratio B_N/B_{N-1}. The other is the problem of a large implicit N-body contact interaction when many particles lie within a region the size of the range of the potential. We regulated this implicit N-body contact interaction on the lattice using a discrete Hubbard-Stratonovich transformation. Using a heat bath algorithm we computed B_N/B_{N-1} for $N\leq 10$. Extrapolating to the large-N limit we found

$$\lim_{N\to\infty}\frac{B_N}{B_{N-1}}=8.3(6). \tag{62}$$

This appears to be in agreement with the value 8.567 found by [3].

While we have measured the large-N limit of B_N/B_{N-1} to within 10%, we relied on large-N similarity under rescaling to keep the finite cutoff errors in check. The z dependence in Fig. 2 suggests that one needs to go beyond leading order to accurately describe all of the physics at large N. This competition between effective field theory expansions and the large-N limit presents an interesting theoretical challenge. Since there are no known physical systems where we can experimentally measure the universal zero range behavior, the coefficients of the higher-dimensional operators must be set by numerical calculations. One technique perhaps is to use numerical renormalization group matching to relate the coefficients of higher-dimensional operators for different values of $mB_2\Lambda^{-2}$. However more study would be needed to see if this is a viable technique.

ACKNOWLEDGMENTS

The author is grateful to Hans-Werner Hammer and Lucas Platter for discussions and for suggesting the problem. The author also thanks Thomas Schäfer for helpful discussions. This work is supported by the U.S. Department of Energy Grant No. DE-FG02-04ER41335.

[1] L. W. Bruch and J. A. Tjon, Phys. Rev. A **19**, 425 (1979).
[2] E. Nielsen, D. V. Fedorov, and A. S. Jensen, Few-Body Syst. **27**, 15 (1999).
[3] H.-W. Hammer and D. T. Son, Phys. Rev. Lett. **93**, 250408 (2004).
[4] J. A. Tjon, Phys. Rev. A **21**, 1334 (1980).
[5] T. K. Lim, S. Nakaichi, Y. Akaishi, and H. Tanaka, Phys. Rev. A **22**, 28 (1980).
[6] L. Vranjes and S. Kilic, Phys. Rev. A **65**, 042506 (2002).
[7] L. Platter, H.-W. Hammer, and U.-G. Meissner, Few-Body Syst. **35**, 169 (2004).
[8] D. Blume, Phys. Rev. B **72**, 094510 (2005).
[9] G. G. Batrouni, V. Rousseau, R. T. Scalettar, M. Rigol, A. Muramatsu, P. J. H. Denteneer, and M. Troyer, Phys. Rev. Lett. **89**, 117203 (2002).
[10] V. W. Scarola and S. Das Sarma, Phys. Rev. Lett. **95**, 033003 (2005).
[11] C. Wu, J. Hu, and S.-C. Zhang, Phys. Rev. Lett. **91**, 186402 (2003).
[12] C. Wu, Phys. Rev. Lett. **95**, 266404 (2005).
[13] J. E. Hirsch, Phys. Rev. B **28**, 4059 (1983).
[14] D. Lee and T. Schafer, Phys. Rev. C **72**, 024006 (2005).
[15] D. Lee, B. Borasoy, and T. Schaefer, Phys. Rev. C **70**, 014007 (2004).
[16] B. Borasoy, H. Krebs, D. Lee, and U. G. Meissner, Nucl. Phys. A **768**, 179 (2006).
[17] D. Lee, Phys. Rev. B **73**, 115112 (2006).